

**Field-induced slow magnetic relaxation and  
magnetocaloric effects in an oxalato-bridged  
gadolinium(III)-based 2D MOF**

Marta Orts-Arroyo, Renato Rabelo, Ainoa Carrasco-Berlanga, Nicolás  
Moliner, Joan Cano, Miguel Julve, Francesc Lloret, Giovanni De Munno,  
Rafael Ruiz-García, Júlia Mayans,\* José Martínez-Lillo\* and Isabel  
Castro\*

## Experimental

### Materials

Oxalic acid (H<sub>2</sub>ox) and gadolinium(III) chloride hexahydrate were of reagent grade and they were used as received.

### Synthetic procedures

[Gd<sup>III</sup><sub>2</sub>(ox)<sub>3</sub>(H<sub>2</sub>O)<sub>6</sub>]<sub>n</sub>·4nH<sub>2</sub>O (**1**). Aqueous concentrated solutions (0.5 mL) of H<sub>2</sub>ox (0.068 g, 0.75 mmol) and GdCl<sub>3</sub>·6H<sub>2</sub>O (0.190 g, 0.5 mmol) were placed at the bottom of each of the two arms of an H-shaped tube and then it was completely filled with water and closed with parafilm. Colorless prisms of **1** were obtained after several weeks of slow diffusion at 50 °C within a thermostated oven. Yield: 0.130 g (68.5%). Anal. calcd (*M*<sub>w</sub> = 758.7 g mol<sup>-1</sup>): C, 9.50; H, 2.66%. Found: C, 9.55; H, 2.61%. IR (KBr, cm<sup>-1</sup>): ν = 3421s (br) (O–H from H<sub>2</sub>O), 1671s and 1317m (C=O from ox).

### Physical techniques

Elemental analyses (C, H) were performed by the Servei Central de Suport a la Investigació Experimental de la Universitat de València. FT-IR spectra were recorded on a Nicolet-5700 spectrophotometer as KBr pellets.

### Magnetic measurements

Direct current (*dc*) and alternating current (*ac*) magnetic measurements were performed on frozen matrix water suspensions of **1** to prevent for partial water loss upon vacuum, with a Quantum Design SQUID (Superconducting Quantum Interference Device) magnetometer and a Quantum Design Physical Property

Measurement System (PPMS). The magnetic susceptibility data were corrected for the diamagnetism of the constituent atoms and the sample holder.

### **Crystallographic data collection and refinement**

X-ray diffraction data of a single crystal of **1** were collected on a Bruker D8 Venture diffractometer with PHOTON II detector by using monochromatized Mo- $K\alpha$  radiation ( $\lambda = 0.71073 \text{ \AA}$ ). The structure was solved by standard direct methods and subsequently completed by Fourier recycling by using the SHELXTL software packages. The obtained models were refined with version 2013/4 of SHELXL against  $F^2$  on all data by full-matrix least squares.<sup>1</sup> A face absorption correction has been done by using empirical/numerical methods (Fig. S11). All non-hydrogen atoms were refined anisotropically. Hydrogen atoms from the coordinated water molecules were set on geometrical positions and refined with a riding model, while those from the crystallisation water molecules were neither found nor fixed. The oxygen atoms from the crystallisation water molecules were disordered. A half occupation factor was assigned within each of the two O4Aw/O4Bw and O5Aw/O5Bw pairs. Due to the disorder of the crystallisation water molecules, their connectivity through hydrogen bonding interactions is very difficult to establish. Yet a possible model is given in Fig. S2 which takes into account reasonable values for the intermolecular hydrogen bonding distances and angles. The graphical manipulations were performed with the CRYSTAL MAKER program.<sup>2</sup>

Crystallographic data (excluding structure factors) for **1** (Table S1) have been deposited with the Cambridge Crystallographic Data Centre as supplementary publication number CCDC–2047766. Copies of the data can be obtained free of

---

<sup>1</sup> *SHELXTL-2013/4*, Bruker Analytical X-ray Instruments; Bruker: Madison, WI, USA, 2013.

<sup>2</sup> *CrystalMaker*, CrystalMaker Software, Bicester, England, 2015.

charge on application to CCDC, 12 Union Road, Cambridge CB21EZ, UK (fax:  
(+44) 1223-336-033; e-mail: [deposit@ccdc.cam.ac.uk](mailto:deposit@ccdc.cam.ac.uk)).

**Table S2.** Summary of crystallographic data for **1**

Formula	C <sub>3</sub> H <sub>10</sub> GdO <sub>1</sub>
<i>M</i> (g mol <sup>-1</sup> )	379.36
Crystal system	Monoclinic
Space group	<i>P</i> 2 <sub>1</sub> / <i>c</i>
<i>a</i> (Å)	11.0564(5)
<i>b</i> (Å)	9.5549(4)
<i>c</i> (Å)	10.0477(4)
$\alpha$ (°)	90
$\beta$ (°)	114.5420(10)
$\gamma$ (°)	90
<i>V</i> (Å <sup>3</sup> )	965.57(7)
<i>Z</i>	4
$\rho_{\text{calc}}$ (g cm <sup>-3</sup> )	2.610
$\mu$ (mm <sup>-1</sup> )	6.917
<i>T</i> (K)	150(2)
Reflect. collcd.	2172
Reflect. obs. [ <i>I</i> > 2 $\sigma$ ( <i>I</i> )]	2041
Data/Restraints/Parameters	2172/6/179
<i>R</i> <sub>1</sub> <sup>a</sup> [ <i>I</i> > 2 $\sigma$ ( <i>I</i> )]	0.0209
<i>wR</i> <sub>2</sub> <sup>b</sup> [ <i>I</i> > 2 $\sigma$ ( <i>I</i> )]	0.0463
<i>S</i> <sup>c</sup>	1.157

<sup>a</sup>  $R_1 = \sum(|F_o| - |F_c|) / \sum|F_o|$ . <sup>b</sup>  $wR_2 = [\sum w(F_o^2 - F_c^2)^2 / \sum w(F_o^2)^2]^{1/2}$ . <sup>c</sup>  $S = [\sum w(|F_o| - |F_c|)^2 / (N_o - N_p)]^{1/2}$ .

**Table S3.** Selected structural, magnetic, and magnetocaloric data for homo- and heteroleptic Gd<sup>III</sup> MOFs with light organic mono- and/or dicarboxylate linkers proposed as cryogenic molecular magnetic coolers.

Entry	Compound <sup>a</sup>	<i>nD</i> <sup>b</sup>	<i>T</i> <sup>c</sup> (K)	$\Delta H^d$ (T)	$-\Delta S_M^e$ (J K <sup>-1</sup> K <sup>-1</sup> )	$\Delta T_{ad}^f$ (K)	$\rho^g$ (g cm <sup>-3</sup> )	$\theta^h$ (K)	<i>T</i> <sub>N</sub> <sup>i</sup> (K)	Ref.
1	Gd <sub>2</sub> (fum) <sub>3</sub> (H <sub>2</sub> O) <sub>4</sub> ·3H <sub>2</sub> O	3D	1.0	2	18.0	7.5	2.52	-7.6	0.2	19
			1.3	5	20.7					
2	Gd(form)(ac) <sub>2</sub> (H <sub>2</sub> O) <sub>2</sub>	1D	0.9	2	37.1	22.5	2.40			7
			1.8	7	45.9					
3	Gd <sub>2</sub> (abdc) <sub>3</sub> (dmf) <sub>4</sub>	3D	1.8	7	29.0		1.42	-0.18		7
4	Gd <sub>2</sub> (ida) <sub>3</sub> ·2H <sub>2</sub> O	3D	2.0	2	22.5		2.48	-0.90		8
			2.0	4	34.9					
			2.0	7	40.6					
			1.9	2	25.7					
5	Gd(form)(bdc)	3D	1.9	2	25.7					9
			1.9	3	33.3					
			2.25	5	42.4					
			2.25	7	46.0					
6	Gd(form) <sub>3</sub>	3D	1.1	2	43.7	22.5	3.86	-0.30	0.8	10
			2.0	7	55.9					
7	Gd <sub>5</sub> (OH) <sub>5</sub> O(CO <sub>3</sub> ) <sub>2</sub> (form) <sub>2</sub> (sq)(H <sub>2</sub> O) <sub>2</sub>	3D	2.0	3	35.5		3.37	-1.64		11
			2.0	7	60.0					
			3.0	9	64.0					
8	Gd <sub>2</sub> (ox) <sub>2</sub> (sq)(H <sub>2</sub> O) <sub>4</sub>	3D	3.0	2	25.0		2.90	-0.18		13
			3.0	7	44.0					
9	Gd <sub>2</sub> (ox) <sub>3</sub> ·6.6H <sub>2</sub> O	2D	2.0	1	11.0		3.00	-0.75		14
			2.0	2	25.3					
			2.0	3	34.4					
			2.0	5	43.0					
			2.0	7	46.6					
10	(H <sub>6</sub> edte)Gd <sub>2</sub> (ox) <sub>4</sub> (H <sub>2</sub> O)	3D	2.0	1	9.9		2.30	-0.09		15
			2.0	3	27.2					
			2.0	9	35.9					
11	Gd(ox)(H <sub>2</sub> PO <sub>2</sub> )(H <sub>2</sub> O) <sub>2</sub>	2D	2.0	3	35.4		2.88	-0.22		16
			2.0	7	46.6					
12	Gd <sub>2</sub> (ox)(fum) <sub>2</sub> (H <sub>2</sub> O) <sub>4</sub> ·4H <sub>2</sub> O	3D	3.0	3	31.0			+0.03		12
			3.0	5	38.4					
			3.0	7	41.6					
13	Gd <sub>2</sub> (ox)(fum) <sub>2</sub>		3.0	3	33.7			-0.28		12
			3.0	5	47.2					
			3.0	7	52.5					

14	Gd <sub>2</sub> (ox) <sub>3</sub> ·10H <sub>2</sub> O (1)	2D	2.0	1	10.2	2.61	-0.27	This work
			2.0	2	21.9			
			2.0	3	29.1			
			2.0	4	33.8			
			2.0	5	37.0			
			2.0	6	39.1			
			2.0	7	40.6			
			2.0	8	41.5			

---

<sup>a</sup> Ligand abbreviations: fum = fumarate; ac = acetate; abdc = 2-amino-1,4-benzenedicarboxylate; ida = iminodiacetate; bdc = 1,4-benzenedicarboxylate; form = formate; sq = squarate; ox = oxalate; H<sub>4</sub>edte = *N,N,N',N'*-tetrakis(2-hydroxy-ethyl)ethylenediamine; fum = fumarate. <sup>b</sup> Structural dimensionality. <sup>c</sup> Value of the temperature. <sup>d</sup> Value of the magnetic field change. <sup>e</sup> Value of the maximum magnetic entropy change (in gravimetric units) estimated from indirect variable-field magnetization or heat capacity measurements. <sup>f</sup> Value of the adiabatic temperature change estimated from direct or indirect or indirect heat capacity measurements. <sup>g</sup> Value of the calculated crystal density. <sup>h</sup> Value of the Weiss temperature obtained from the fitting of the magnetic susceptibility data to the Curie-Weiss law. <sup>i</sup> Value of the Néel temperature for the long-range antiferromagnetic order.

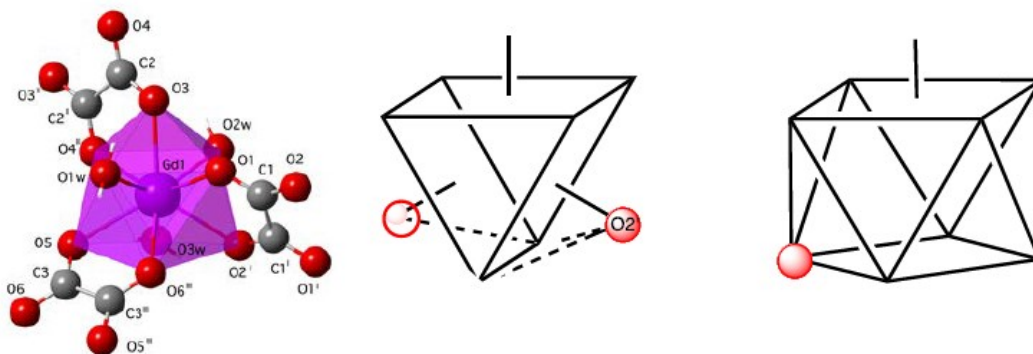


**Fig. S1.** Coordination environment around each crystallographically independent Gd(III) ion for **1** with the atom numbering scheme [symmetry code: IV = 1-x, -y, 1-z]. The two alternative ideal tricapped trigonal prism (TCTPR) and monocapped square antiprism (CSAPR) polyhedra are shown for comparison. The grey arrows represent the simple pathway for the structural transformation between each other.

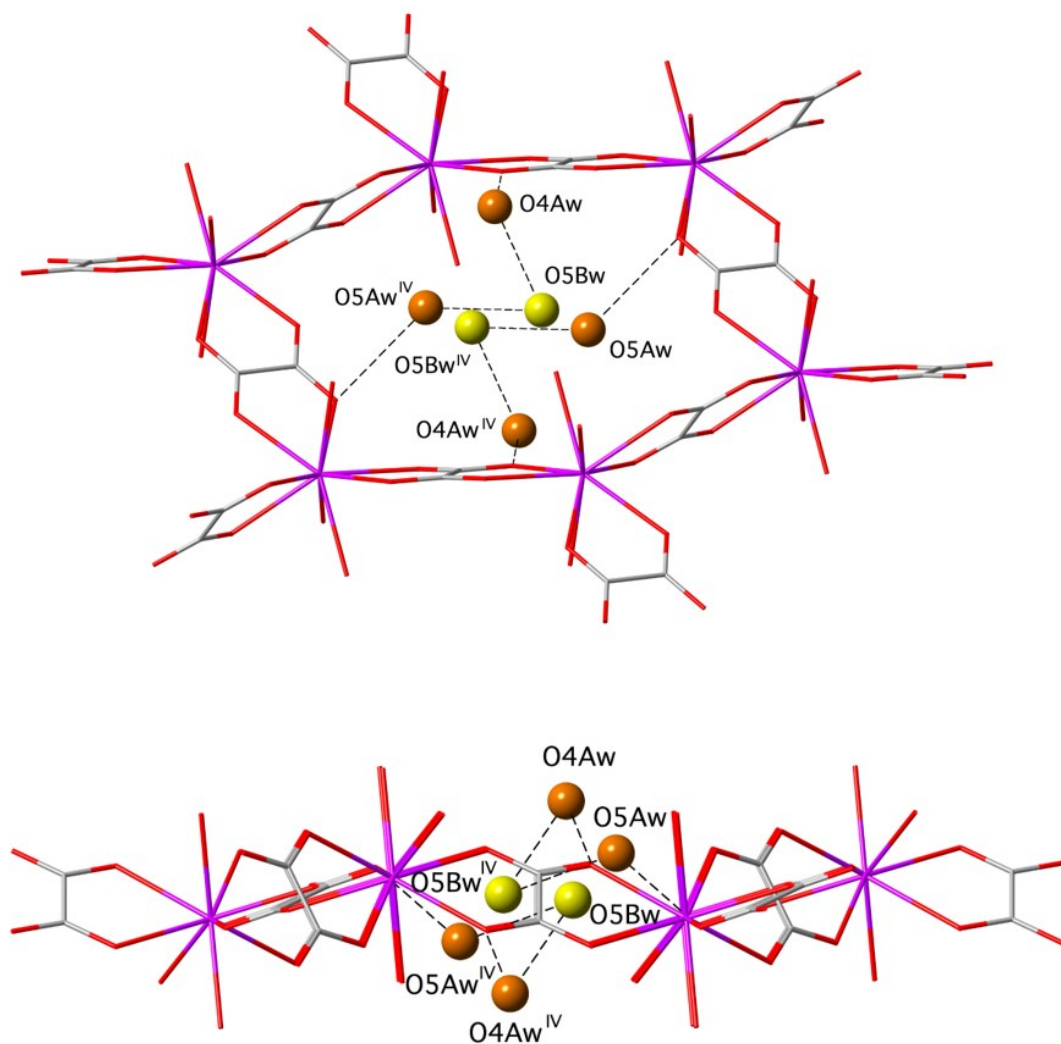


**Fig. S2** Top and front views of the hexagonal ring of the neutral oxalato-bridged gadolinium(III) hexagonal layer of **1** with the atom numbering scheme showing the hydrogen-bonded crystallization water molecules occupying the intra- and interlayer spaces. The two sets of disordered crystallisation water molecules with half-occupancy factors are represented by yellow and orange spheres. Hydrogen bonds are shown as dashed lines.

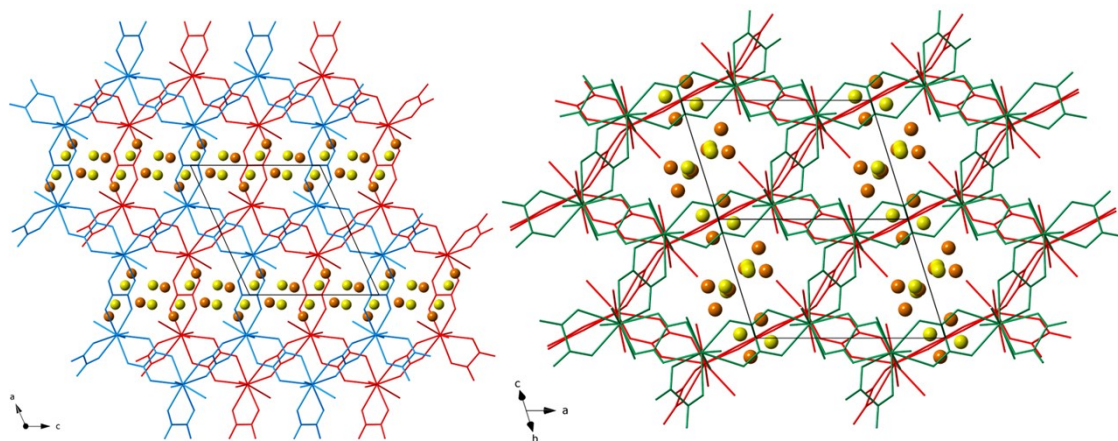


**Fig. S3** Projection views of the crystal packing of **1** along the [010] (left) and [011] (right) directions. The two sets of disordered crystallization water molecules with half-occupancy factors are represented by yellow and orange spheres.

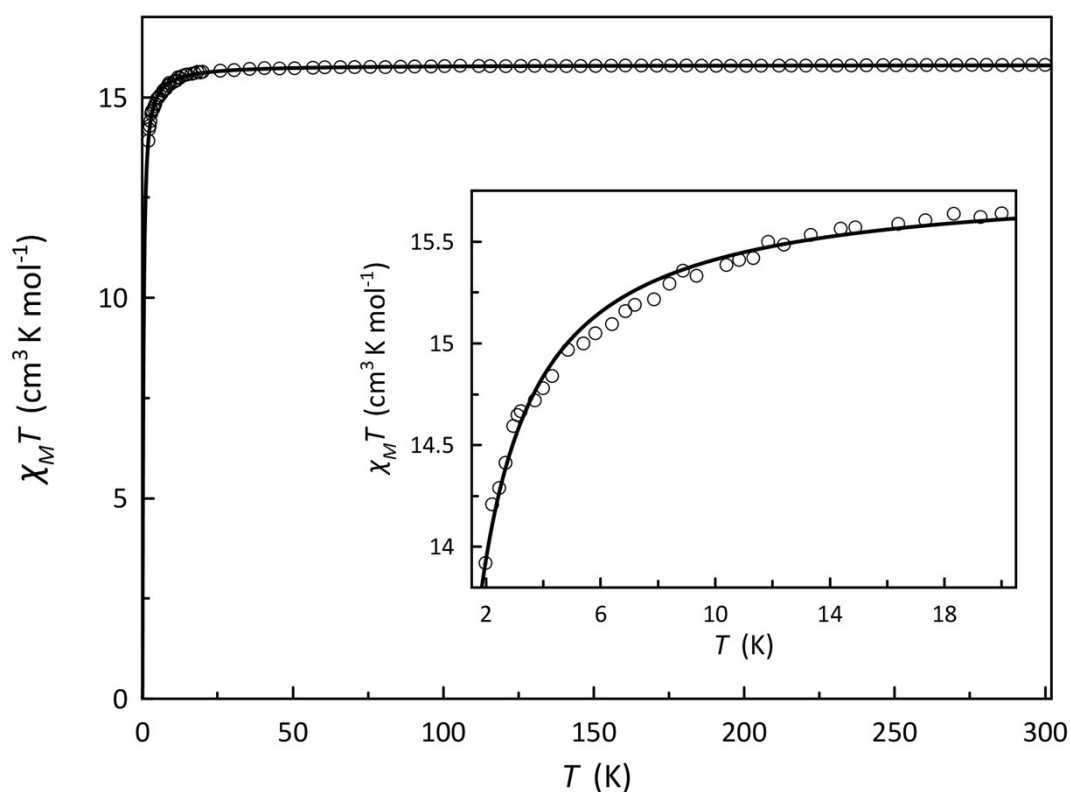


**Fig. S4.** Temperature dependence of  $\chi_M T$  for **1** under applied *dc* magnetic fields of  $H = 0.025$  ( $T \leq 20$  K) and 5 T ( $T > 20$  K). Solid line is the best-fit curve through the Monte Carlo simulations (see text).

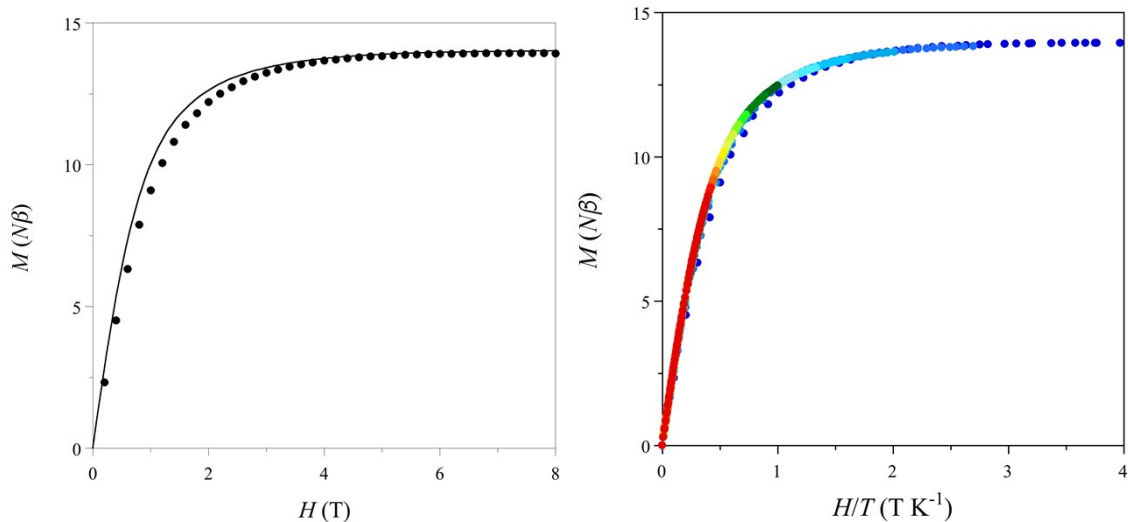


**Fig. S5.** Magnetisation curve (left) at  $T = 2$  K and reduced magnetisation curves (right) in the temperature range of  $T = 2$ – $20$  K (blue to red) for **1**. Solid line is the simulated curve through the Brillouin function (see text).

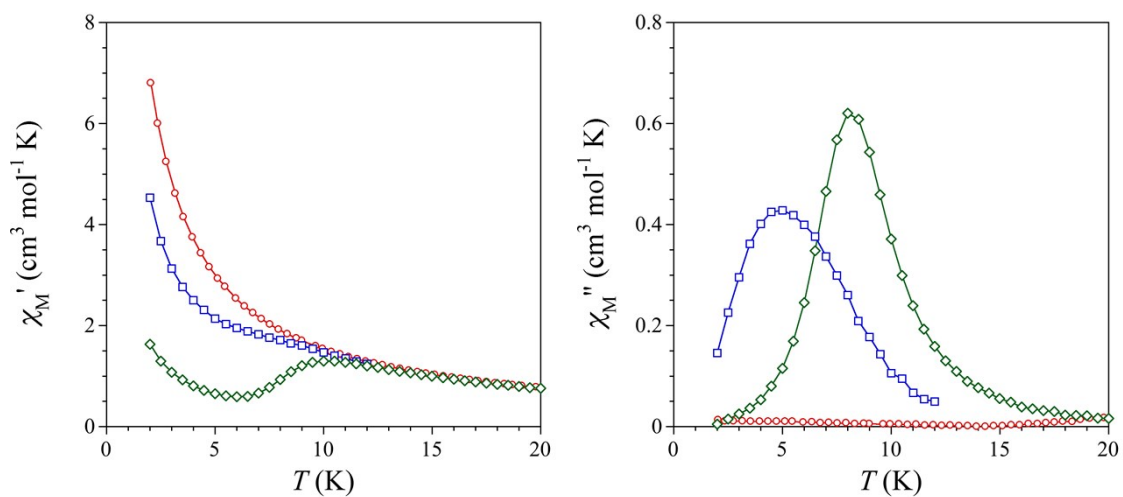


**Fig. S6** Temperature dependence of  $\chi_M'$  (left) and  $\chi_M''$  (right) for **1** at  $\nu = 1000$  Hz of the  $\pm 4$  Oe oscillating field and under an applied static magnetic field of  $H = 0$  ( $\circ$ ),  $0.1$  ( $\bullet$ ), and  $0.25$  T ( $*$ ). Solid lines are only eye-guides.

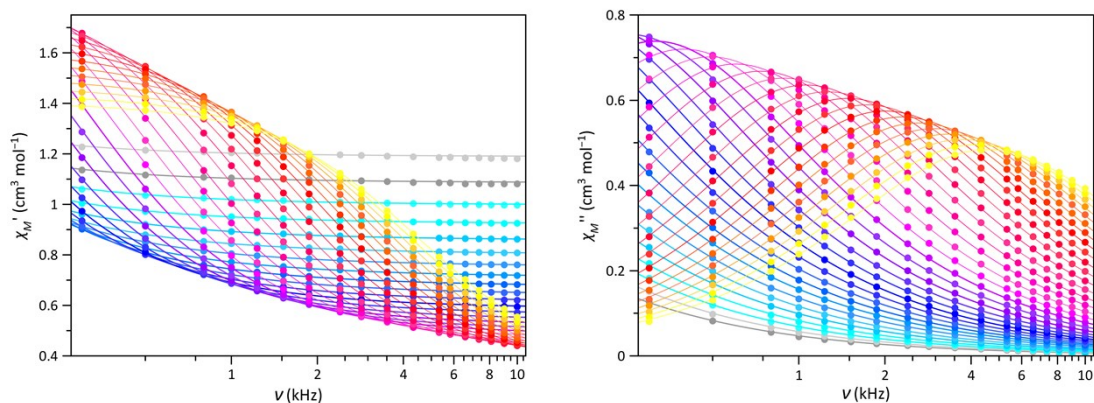


**Fig. S7** Frequency dependence of  $\chi_M'$  and  $\chi_M''$  of **1** in the temperature range of  $T = 2.5$ – $11.0$  K (gray to yellow) at  $H = 0.25$  T. Solid lines are the best-fit curves through the generalised Debye model (see text).

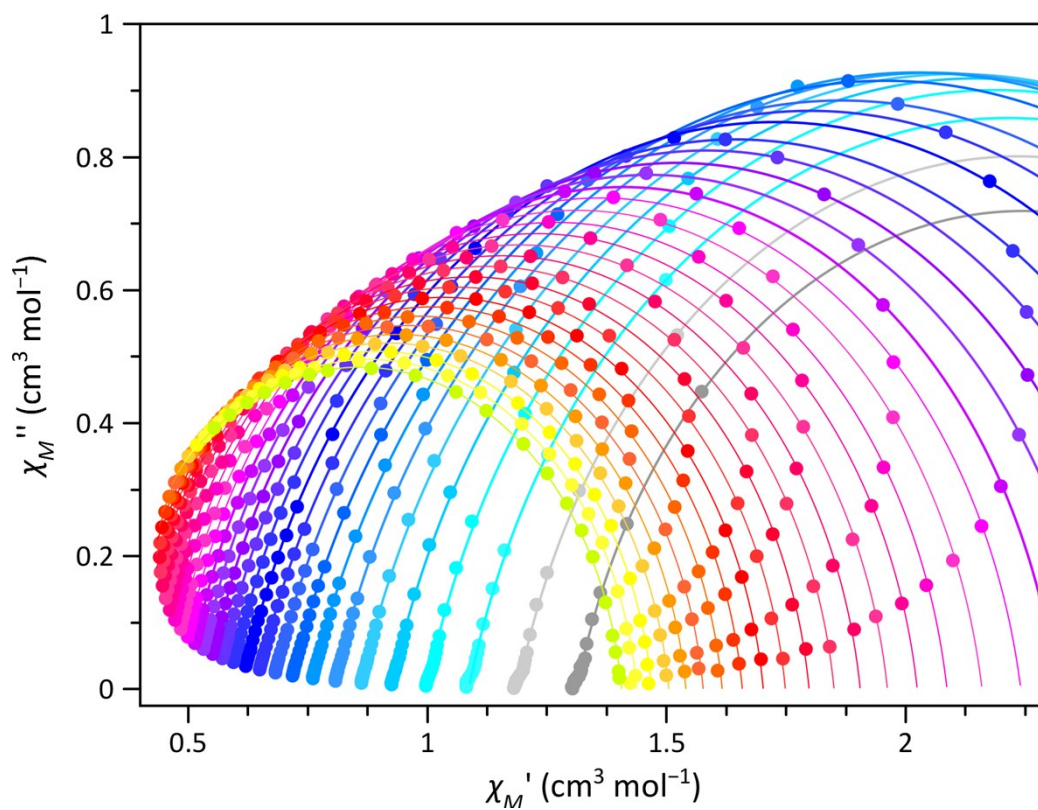


**Fig. S8** Argand plots of **1** in the temperature range of  $T = 2.5$ – $11.0$  K (grey to yellow) at  $H = 0.25$  T. The solid lines are the simulated curves through the generalised Debye model (see text).

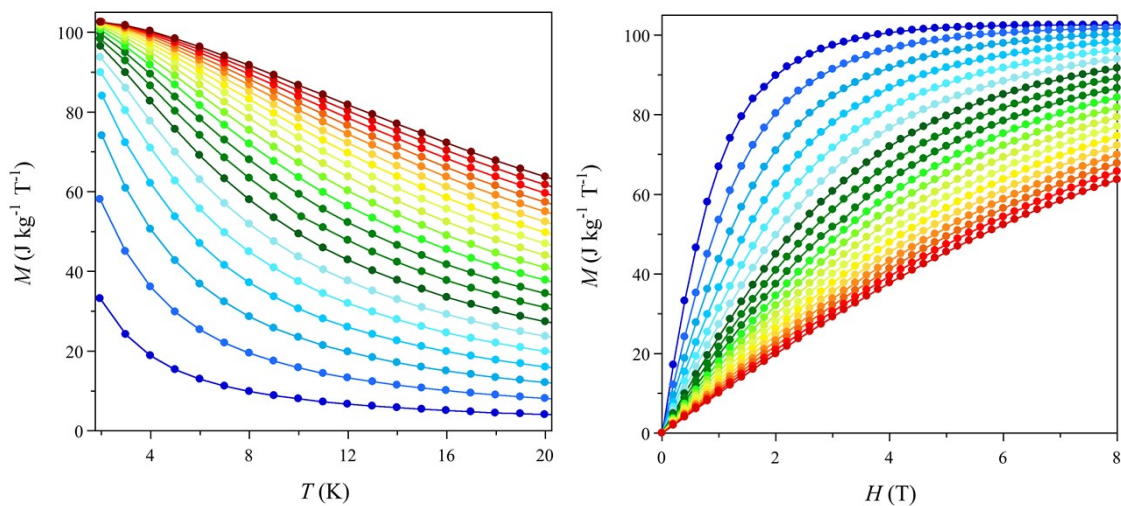


**Fig. S9** Temperature (left) and field dependence (right) of  $M$  for **1** in the magnetic field and temperature ranges of  $H = 0\text{--}8$  T and  $T = 2\text{--}20$  K (blue to red), respectively.

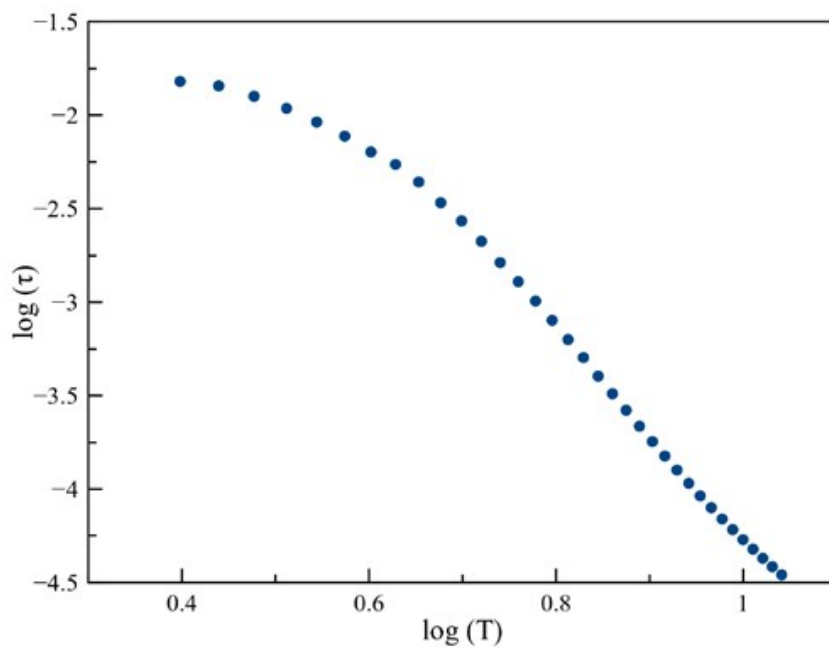


**Fig. S10.** Temperature dependence of the relaxation time of compound **1** represented in a log-log plot. In the representation is evident the two different slopes regime corresponding to the Raman and IK contributions (see text).

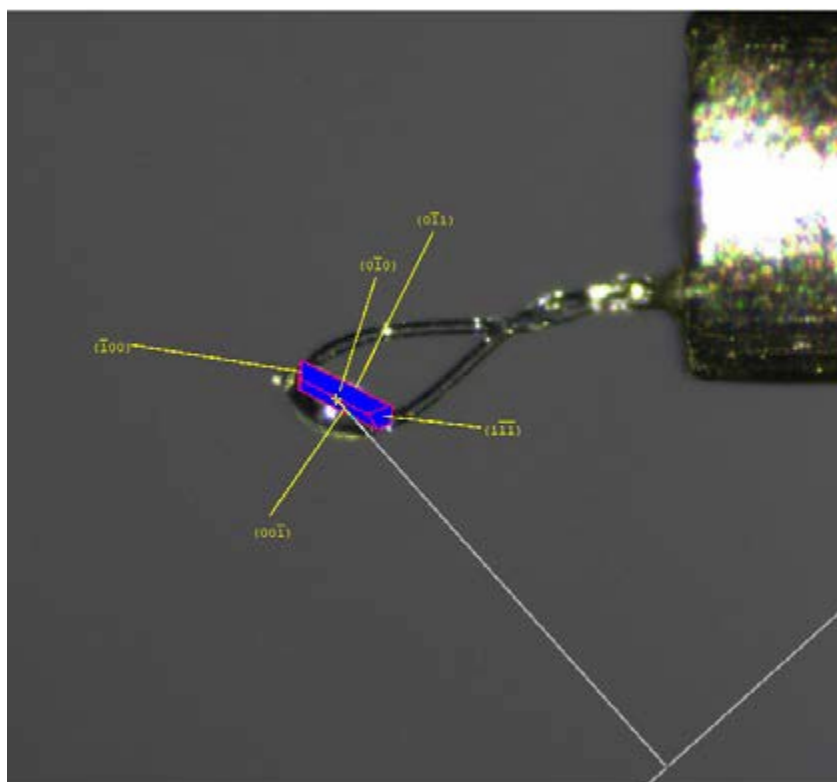


**Fig. S11.** Face indexing of a crystal of 1, mounted on a goniometer head and indicating the crystallographic planes (dimensions: 0.21 x 0.07 x 0.04 mm<sup>3</sup>).